Proceedings of the 5th WSEAS Int. Conf. on Signal Processing, Robotics and Automation, Madrid, Spain, February 15-17, 2006 (pp113-118)

Visual Servoing for a Hyperredundant Robot

Mircea Ivănescu*, Dorian Cojocaru*, Nirvana Popescu**, Decebal Popescu** and Răzvan Tudor Tănasie*

*Mechatronics Department, University of Craiova,
**Computers Department, University POLITEHNICA Bucharest,
Bulevardul Decebal, Nr. 107, 200440, Craiova
ROMANIA

Abstract: - The control problem of a tentacle manipulator using a robust 3 D visual servoing is presented. The theoretical model of this class of arms is studied. Servoing is based on binocular vision obtained from two cameras that ensure a continuous measure of the arm parameters. The control errors function is built in 3D cartesian space from the visual information obtained in the two image planes. The 2D errors are determined as shape errors, they are calculated as the differences between the actual and desired continuous angle values. A spatial error is determined and a control law is discussed. Computer simulations and real 3-D experiments are presented in order to show the applicability of the method.

Key-Words: Videoservoing, Robot Control, Hyperredundant Manipulator.

1 Introduction

An ideal tentacle manipulator is a non-conventional robotic arm with an infinite mobility. It has the capability of takeing sophisticated shapes and of achieving any position and orientation in a 3D space. These systems are also known as hyperredundant manipulators and, over the past several years, there has been a rapid expanding interest in their study and construction.

The control of these systems is very complicated and a great number of researchers tried to offer solutions for this difficult problem. In [1] it analyses the control by cables or tendons meant to transmit forces to the elements of the arm in order to closely approximate the arm as a truly continuous backbone. Also, Mochiyama has investigated the problem of controlling the shape of an HDOF rigid-link robot with two-degree-of-freedom joints using spatial curves [7], [8]. Important results were obtained by Chirikjian and Burdick [3] – [6] who laid the foundations for the kinematic theory of hyperredundant robots. Their results are based on a "backbone curve" that captures the robot's macroscopic geometric features.

The inverse kinematic problem is reduced to determining the time varying backbone curve behaviour. New methods for determining "optimal" hyper-redundant manipulator configurations based on a continuous formulation of kinematics are developed. In [2], Gravagne analysed the kinematic model of "hyper-redundant" robots, known as "continuum" robots. Robinson and Davies [8] present the "state of art" of continuum robots, outline their areas of application and introduce some control issues. The great number of parameters, theoretically an infinite one, makes very difficult the use of classical control methods and the conventional transducers for position and orientation.

In this paper the method of image-based servoing [12,15] for a hyperredundant arm is studied. Servoing is based on binocular vision. A continuous measure of the arm parameters, derrived from the real-time computation of the binocular optical flow over the two images, is compared with the desired position of the arm.

The control error function is built in 3D cartesian space using the visual information obtained from two cameras in two image planes [13]. The two 2D errors obtained in the two image planes are determined by the two differences between the actual and desired continuous angle values that define the projections of the arm shape. The plane errors can be considered as errors of the arm shape. These errors are used to calculate the spatial error and a control law is synthesized.

For the closed-loop control system, the stability is proven by using the Lyapunov second method. The error function is computed virtually in the image spaces and the fact that no calibration (camera parameters) is required allows the synthesis of a more robust control laws.

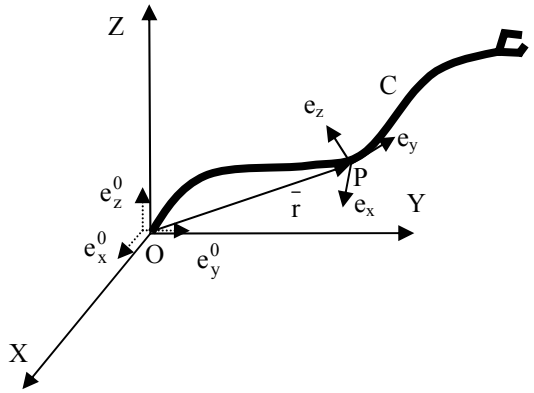

Figure 1.

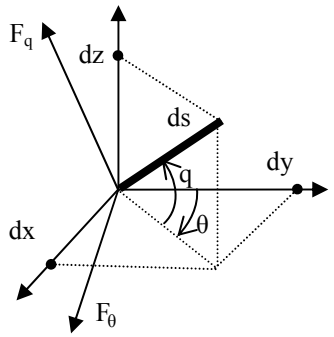

Figure 2.

2 Background

Consider a 3D hyperredundant robot with a three dimensional Cartesian coordinate frame called the robot coordinate frame whose axes are labeled X, Y, Z. The mechanical structure represents an ideal arm, with an uniform distributed mass and torque, with ideal flexibility that can take any arbitrary shape (Fig. 1). We will neglect friction and structure damping. The essence of the model is a 3 – dimensional backbone curve C that is parametrically described by a vector $r(s) \in \Re^3$ and an associate frame $\Phi(s) \in \Re^3$ whose columns create the frame base (Fig. 2) [2,3]. The independent parameter s is related to the arc length from the origin of the curve C. The position of a point s on the curve C is defined by the position vector,

$$\bar{r} = \bar{r}(s) \tag{2.1}$$

where $s \in [0,l]$. For a dynamic motion, the time variable is introduced, $\bar{r} = \bar{r}(s,t)$. The parametrisation of the curve C is based on two "continous angle" $\theta(s)$ and q(s) [3,5] (Fig. 2). At each point $\bar{r}(s,t)$, the robot's orientation is given by a right-handed orthonormal basis vector $\{\bar{e}_x, \bar{e}_y, \bar{e}_z\}$ and its origin coincides with the point $\bar{r}(s,t)$. The set of backbone frames can be parametrized as

$$\Phi^s(t) = \left(\bar{e}_x(s,t), \bar{e}_y(s,t), \bar{e}_z(s,t)\right) \tag{2.2}$$

The pointer vector on curve C is given by

$$\bar{r}(s,t) = \left(x(s,t), y(s,t), z(s,t)\right)^T \tag{2,3}$$

where

$$x(s,t) = \int_0^s \sin\theta(s',t) \cdot \cos q(s',t) \cdot ds'$$

$$y(s,t) = \int_0^s \cos\theta(s',t) \cdot \cos q(s',t) \cdot ds' \tag{2.4}$$

$$z(s,t) = \int_0^s \sin q(s',t) \cdot ds'$$

where $s' \in [0,s]$.

We adopt the following interpretation [6,7]: at any point s the relation (2.4) determines the current position and Φ^s determines the robot's orientation and the robot's shape is defined by the behaviour of function $\theta(s)$ and q(s). The robot "grows" from the origin by integrating to get $\bar{r}(s,t)$, $s \in [0,l]$. By using this definition, two position of the hyperredundant can be defined by a curve C as

$$C : (\theta(s), q(s)) \qquad , s \in [0,l] \tag{2,5}$$

The motion and orientation of the arm are given by the distributed forces on the legth of the arm, $F_\theta(s,t)$ and $F_q(s,t)$ that rotate the element ds in the planes of the angles $\theta(s)$ and q(s), respectively. The manipulator model is considered as a distributed parameter system defined on a fix spatial domain [0,l] and the spatial coordinate is s. The dynamic model of this manipulator with hyperredundant configuration can be obtained from Hamilton partial differential equations [10].

$$\frac{\partial \omega(t,s)}{\partial t} = \frac{\delta H}{\delta \nu(t,s)}$$
$$\frac{\partial \nu(t,s)}{\partial t} = -\frac{\delta H}{\delta \omega(t,s)} + F(t,s) \tag{2.6}$$

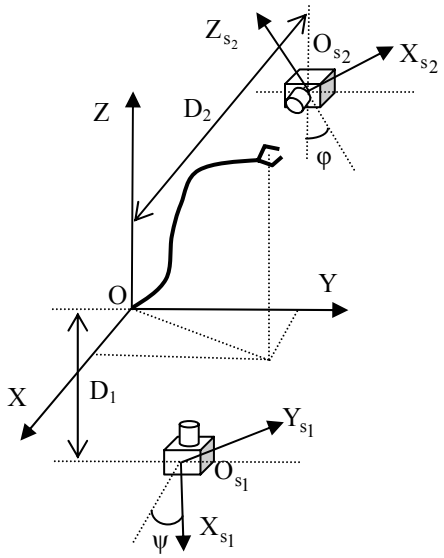

Figure 3

where ω and ν are the generalised coordinates and momentum derivated respectively and $\delta(.)/\delta(.)$ denotes a functional partial derivative.

The state of the system ot any fixed time t is specified by the set $(\omega(t,s),\nu(t,s))$, where $\omega \in [\theta \quad q]^T$ The control force is a distributed force along the arm

$$F = \begin{bmatrix} F_\theta & F_q \end{bmatrix}^T \tag{2.7}$$

2 Camera System

In the Appendix 1 the dynamic model of the 3D spatial hyperredundant arm is determinated. Two video cameras provide two images of the whole robot workspace. The two images planes are parallel with XOY and ZOY planes from robot coordinate frame, respectively (Fig. 3). The cameras provide the images of the scene stored in the frame grabber's video memory being displayed on the computer screens. Related to the image planes, two dimensional coordinate frames, called screen coordinate frames or image coordinate systems are defined. Denote X_{S_1}, Y_{S_1} and Z_{S_2}, Y_{S_2}, respectively, the axes of the two screen coordinate frames provided by the two cameras. The spatial centers for each camera are located at the distances D_1 and D_2, with respect to the XOY and ZOY planes, respectively. The orientation of the cameras arround the optical axes with respect to the robot coordinate frame, are noted with ψ and φ, respectively. A point P in the coordinate frame is

$$P=[\, x,\, y,\, z]^T \tag{3.1}$$

The description of a point P in the two screen coordinate frames are denoted by

$$P_{S_1} = [\, x_{S_1}, y_{S_1}\,] \tag{3.2}$$

$$P_{S2} = [\, z_{S_2}, y_{S_2}\,] \tag{3.3}$$

Geometric optics are used to model the mapping between the robot Cartesian space and the screen coordinate systems. We assume that the quantization and the lens distortion effects are negligible. The description of the point P=[x, y, z]^T in the robot coordinate frame is given in terms of screen coordinate frames as [9]

$$\begin{bmatrix} x_{s_1} \\ y_{s_1} \end{bmatrix} = \alpha_1 \cdot \frac{\lambda_1}{\lambda_1 - (D_1 + x)} \cdot R(\phi) \cdot \cdot \left\{ \begin{bmatrix} x \\ y \end{bmatrix} - \begin{bmatrix} o_{11} \\ o_{12} \end{bmatrix} \right\} + \begin{bmatrix} c_{x_1} \\ c_{y_1} \end{bmatrix} \tag{3.4}$$

for the $Z_{S_1} O_{S_1} Y_{S_1}$ frame and

$$\begin{bmatrix} z_{s_2} \\ y_{s_2} \end{bmatrix} = \alpha_2 \cdot \frac{\lambda_2}{\lambda_2 - (D_2 + x)} \cdot R(\phi) \cdot \cdot \left\{ \begin{bmatrix} z \\ y \end{bmatrix} - \begin{bmatrix} o_{21} \\ o_{22} \end{bmatrix} \right\} + \begin{bmatrix} c_{z_2} \\ c_{y2} \end{bmatrix} \tag{3.5}$$

for the $Z_{S_2} O_{S_2} Y_{S_2}$ frame, where $[c_{x_1}, c_{y_1}]^T$ and $[c_{z_2}, c_{y_2}]^T$ the image centers, α_1 and α_2 are the scale factors of the length units in the front image planes given in pixel/m [9,15], R(ψ) and R(ϕ) are the rotation matrices generated by clockwise rotating the cameras about their optical axes by ψ and ϕ radians, respectively, and $[o_{11}, o_{12}]^T$ and $[o_{21}, o_{22}]^T$ represent the distances between the optical axes and the XOY and ZOY planes, respectively.

In Fig. 4 the screen images of the two cameras are presented. From the relations (3.4), (3.5), we obtain

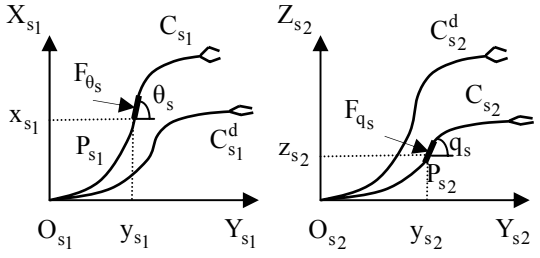

Figure 4

$$\begin{bmatrix} \Delta x_{s_1} \\ \Delta y_{s_1} \end{bmatrix} = \alpha_1 \cdot \frac{\lambda_1}{\lambda_1 - (D_1 + x)} \cdot \begin{bmatrix} \Delta x \\ \Delta y \end{bmatrix} \quad (3.6)$$

$$\begin{bmatrix} \Delta z_{s_2} \\ \Delta y_{s_2} \end{bmatrix} = \alpha_2 \cdot \frac{\lambda_2}{\lambda_2 - (D_2 + x)} \cdot \begin{bmatrix} \Delta z \\ \Delta y \end{bmatrix} \quad (3.7)$$

and the orientation angles for each plane will be

$$tg\theta_s = \frac{\Delta x_{s_1}}{\Delta y_{s_1}} = \frac{\Delta x}{\Delta y} = tg\theta \quad (3.8)$$

hence

$$\theta_s(s') = \theta(s) \quad , s \in [0,l] \, , s' \in [0,l'] \quad (3.9)$$

for the plane $Z_{S_1} O_{S_1} Y_{S_1}$ and $tgq_s = \frac{\Delta z_{s_2}}{\Delta y_{s2}} = \frac{\Delta z}{\Delta y}$

This relation allows the computation of the orientation angle q_s in the plane $Z_{S_2} O_{S_2} Y_{S_2}$

$$tgq_s(s'') = tgq(s) \cdot \frac{1}{\cos\theta(s)}$$
$$s \in [0,l] \, , s'' \in [0,l''] \quad (3.10)$$

where, s', s'' and l', l'' represent the projections of the variable s and the length l in the two planes, respectively. The projection of the forces on the two planes can be easily inferred from the Fig. 2 and the relations (3.8)-(3.10),

$$F_{\theta_s} = F_\theta \quad (3.11)$$

$$F_{q_s} = F_q \cdot \sqrt{\cos^2 q + \sin^2 q \cdot \cos^2 \theta} \quad (3.12)$$

3 Servoing system

The control system is an image – based visual servo control where the error control signal is defined directly in terms of image feature parameters. The desired position of the arm in the robot space is defined by the curve Cd,,

$$C : (\theta^d(s), q^d(s)) \quad , s \in [o,l] \quad (4.1)$$

or, in the two image coordinate frames $Z_{S_1} O_{S_1} Y_{S_1}$ and $Z_{S_2} O_{S_2} Y_{S_2}$, by the projection of the curve C,

$$C_{s_1}^d : (\theta_s^d(s')) \quad , s' \in [0,l'] \quad (4.2)$$

$$C_{s_2}^d : (q_s^d(s'')) \quad , s'' \in [0,l''] \quad (4.3)$$

Define the motion errors as

$$e_\theta(t,s) = \theta(t,s) - \theta_d(s) \quad , s \in [0,l] \quad (4.4)$$

$$e_q(t,s) = q(t,s) - q_d(s) \quad , s \in [0,l] \quad (4.5)$$

or, in the image coordinate frames, by $s' \in [0,l']$, $s'' \in [0,l'']$

$$e_{\theta_s}(t,s') = \theta_s(t,s') - \theta_s^d(s') \quad (4.6)$$

$$e_{q_s}(t,s'') = q_s(t,s'') - q_s^d(s'') \quad (4.7)$$

The global control system is presented in Fig. 5. The control problem of this system is a direct visual servocontrol but we do not use the clasical concept of the position control where the error between the robot end-effector and target is minimized. In this paper we will use the control of the curve's shape in each point of the mechanical structure. The method is based on the particular structure of the system defined as a "backbone with two continuous angles $\theta(s)$ and q(s)". The control of the system is based on the control of the two angles $\theta(s)$ and q(s). These angles are measured directly or indirectly. The angle $\theta(s)$ is measured dircetly by the projection on the image plane $Z_{S_1} O_{S_1} Y_{S_1}$ (relation 3.9) and q(s) is computed from the projection on the image plane $Z_{S_2} O_{S_2} Y_{S_2}$ (relation 3.10). The stability of the closed-loop system is proven by the Lyapunov's second method but, in order to avoid the complex problems derived from using the nonlinear derivation integral model, in this paper a method based on the energy-work relationship [14] will be developed.

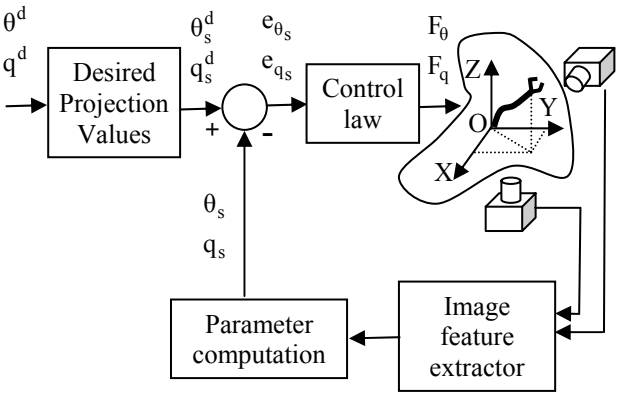

Figure 5

Propostion: The closed-loop hyperredundant arm system is stable if the control law is given by

$$F_\theta(s,t) = -k_\theta^1(s)\cdot e_{\theta_s}(s',t) - k_\theta^2(s)\cdot \dot{e}_{\theta_s}(s',t) \quad (4.8)$$

$$F_q(s,t) = -k_q^1(s)\cdot\left[tg^{-1}(\cos\theta_s(s',t))\cdot \cdot tgq_s(s'',t) - q^d(s)\right] \quad (4.9)$$

where $s' \in [0,l']$, $s'' \in [0,l'']$ and $k_\theta^1(s), k_\theta^2(s), k_q^1(s)$ are positive coefficients of the control law for all $s \in [0,l]$. The parameter of the control law (4.8), (4.9), can be inferred from the image feature extraction of the two planes. The parameters e_{θ_s} can be directly calculated from equation 4.6 and $\dot{e}_{\theta_s}$ can be indirectly computed. Also θ_s, qs and q_s^d are evaluated directly from the trajectory projections. We remark that the control law (4.8), (4.9) represents a robust control, independent of the camera parameters. No intrinsec camera parameters are assumed known.

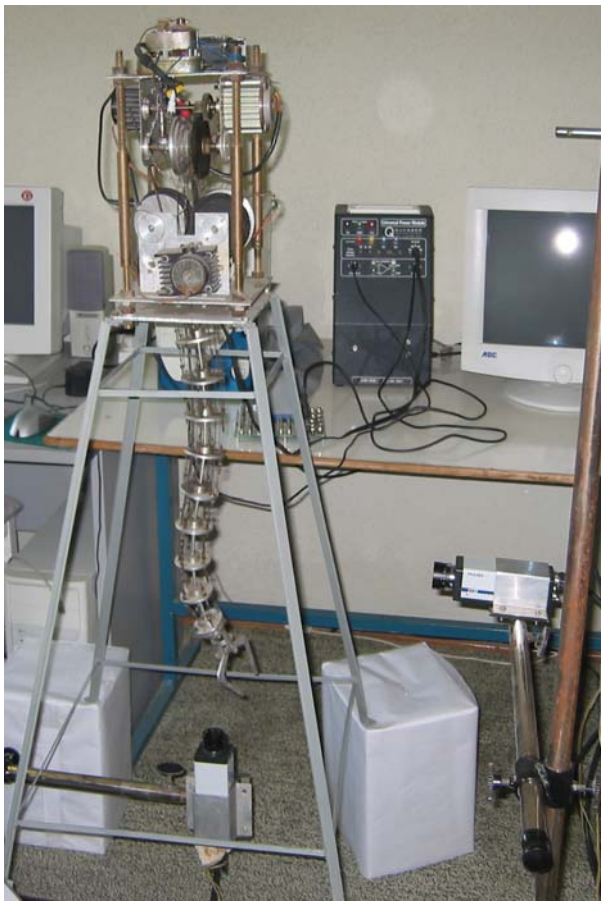

Figure 6

5 Experimental model

We used an experimental model presented in Fig. 6. The manipulator has a very simple design consisting of a highly elastic rod and its "backbone" with antagonic cable pairs periodically able to exert moments on the backbone to deform its shape. [1]. Although this is a truly continuous device, as a hyperredundant model, it is only actuated with 6 degrees of freedom. The driving system consists of 6 DC motors that offer the advantage of a good closed loop system. An Unversal Power Module – Quancer is used in order to implement the control of driving system. The video system is based on DT3162 frame grabber from Data Translation. Two Pulnix TMC 76S CCD cameras with Vista 4.8 mm F1.8 lens were mounted in perpendicular planes offering the input for the frame grabber. The image processing tasks are performed using Global LAB Image2 from Data Translation. The robot control algorithms are implemented in a C++ program running on a Pentium IV PC. In order to facilitate the image feature extraction, a set of markers are placed on joints along the backbone structure (Fig. 7). The localization of the markers in the image planes assures the identification of the curves C_{s_1} and C_{s_2} in the planes $X_{S_1}O_{S_1}Y_{S_1}$ and $Z_{S_2}O_{S_2}Y_{S_2}$ respectively. In the Fig. 8 is shown an example of curve C_{s_2} and the desired curve $C_{s_2}^d$.

6 Conclusions

In this paper the method of image-based servoing for a hyperredundant arm is studied. Servoing is based on binocular vision. A continuous measure of the arm parameters, derrived from the real-time computation of the binocular optical flow over the two images, is compared with the desired position of the arm. The control error function is built in 3D cartesian space using the visual information obtained from two cameras in two image planes. The two 2D errors obtained in the two image planes are determined by the two differences between the actual and desired continuous angle values that define the projections of the arm shape. The plane errors can be considered as errors of the arm shape. These errors are used to calculate the spatial error and a control law is synthesized. For the closed-loop control system and a control law the stability is proven by using the Lyapunov second method. The error function is computed in the image spaces virtually and no calibration is required allowing the synthesis of more robust control laws.

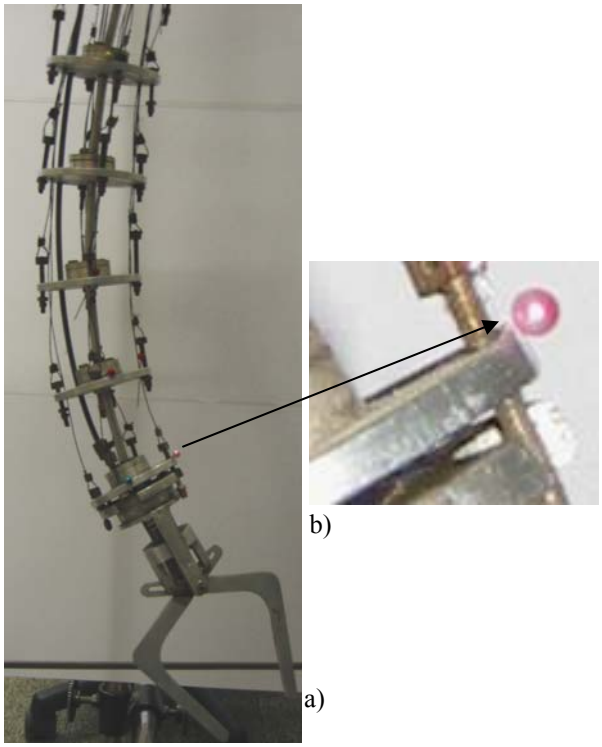

b)

a)

Figure 7
a) $Z_{s_1} O_{s_2} Y_{s_2}$ image plane
b) Detail of position marker

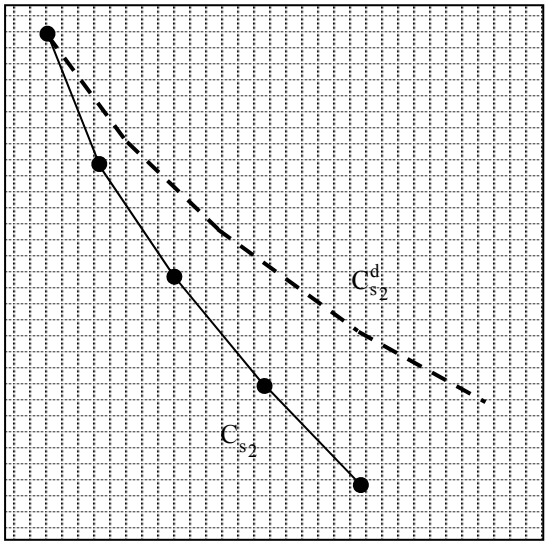

Figure 8 Postprocessed image

References

[1] Hemami, A., 1984 "Design of Light Weight Flexible Robot Arm", Robots 8 Conference Proceedings, Detroit, USA, pp. 1623-1640.

[2] Gravagne, Ian A., Walker, Ian D., 2000, "On the Kinematics of Remotely – Actuated Continuum Robots", Proc. 2000 IEEE Int. Conf. on Rob. and Autom, San Francisco, pp. 2544-2550.

[3] Chirikjian, G. S., Burdick, J. W., 1990, "An Obstacle Avoidance Algorithm for Hyper-redundant Manipulators", Proc. 2000 IEEE Int. Conf. on Rob. and Automation, Cincinnati, Ohio, pp. 625-631.

[4] Chirikjian, G. S., Burdick, J. W., 1992, "Kinematically Optimal Hyper-redundant Manip Config", Proc. 2000 IEEE Int. Conf. on Rob and Autom, Nice, pp. 415-420.

[5] Chirikjian, G. S., 1993, "A General Numerical Method for Hyper-redundant Manipulator Inverse Kinematics", Proc. 2000 IEEE Int. Conf. on Rob and Autom., Atlanta, pp. 107-112.

[6] Chirikjian, G. S., Burdick, J. W., 1995, "Kinematically Optimal Hyper-redundant Manipulator Configurations", IEEE Trans. Rob and Autom, 11, no. 6, pp. 794-798.

[7] Mochiyama, H., Kobayashi, H., 1999, "The Shape Jacobian of a Manipulator with Hyper Degrees of Freedom", Proc. 1999 IEEE Int. Conf. on Rob. and Automation, Detroit, pp. 2837-2842.

[8] Robinson, G., Davies, J. B. C., 1999, "Continuum Robots – a State of the Art ", Proc. 1999 IEEE Int. Conf. on Robotics and Automation, Detroit, Michigan, pp. 2849-2854.

[9] Kelly, R., "Robust Asymptotically State Visual Servoing of Planor Robots", IEEE Trans. and Robotics and Automation, vol. 22, Nr. 15, oct. 1996, pp. 759-765.

[10] Wang, P. K. C., 1965, "Control of Distributed Parameter Systems", in Advance in Control Syst, by C. T. Leondes, Academic Press.

[11] Ivanescu, M., 2002, "Position Dynamic Control for a Tentacle Manipulator", Proc. IEEE Int. Conf. on Rob and Automation, Washington, A1-15, 1531-1539.

[12] Hutchinson, S., Hager, G. D., Corke, P. F., "A Tutorial on Visual Servor Control", IEEE Trans. on Robotics and Automation, vol. 12, Nr. 15, oct. 1996, pp. 651-670.

[13] Grosso, E., Metta, G., Oddera, A., Sandrini, G., "Robust Visual Servoing in 3D Reaching Tasks", IEEE Trans. on Rob and Autom, vol. 12, Nr. 15, oct. 1996, pp. 732-742.

[14] Wang, Z. P., Ge, S. S., Lee, T. H., "Non-Model-Based Robust Control of Multi-Link Smart Material Robots", Asian Conference on Robotics and Its Application, Singapore, pp. 268-273, 2001.

[15] Adachi, J., Sato, J., (2004), "Uncalibrated Visual Servoing from Projectiove Reconstruction of Control Values", Proceedings of the 17th International Conf on Pattern Recognition (ICPR '04), pp. 1051-4651/04.

[16] Pressigout, M., E. Marchand, (2004), "Model-free Augmented Reality by Virtual Visual Servoing", Proceedings of the 17th International Conference on Pattern Recognition (ICPR '04), pp. 1051-4651/04.